Robust Fractional Order Control of Under-actuated Electromechanical System

Mohammad Goodarzi[1*]
[1]Department of Electrical Engineering, Faculty of Engineering, Garmsar branch, Islamic Azad University, Garmsar, Iran
*Email of corresponding author: m_goodarzi181@yahoo.com
Received: December 20, 2015 ; Accepted: June 9, 2016

Abstract
This paper presents a robust fractional order controller for flexible-joint electrically driven robots under imperfect transformation of control space. The proposed approach is free from manipulator dynamics, thus free from problems associated with torque control strategy in the design and implementation. As a result, the proposed controller is simple, fast response and superior to the torque control approaches. It can guarantee robustness of control system to both structured and unstructured uncertainties associated with robot dynamics. The control method is verified by stability analysis. Simulation results on a two-link actuated flexible-joint robot show the effectiveness of the proposed control approach.

Keywords
Robust Fractional Order Control, Electrically Driven Robots, Flexible-Joint Robots

1. Introduction

Although torque controllers are frequently used for controlling robotic manipulators [1-6], the role of actuator dynamics considered by voltage control in some cases cannot be neglected. Indeed, torque controllers have some limitations coming from practical point of view as follows:

-A torque control law cannot be given directly to the torque inputs of an electrical manipulator [7]. Because, physical control variables are electrical signals to the actuators not the torque vector applied to the robot joints.

-The dynamics of motors and drives are excluded in the torque control strategies, [8], while the actuator dynamics are often a source of uncertainty due to e.g. calibration errors, or parameter variation from overheating and changes in environment temperature.

-The control problem becomes hypersensitive when tracking the fast trajectories is demanded. Therefore, control performance degrades quickly as speed increases.

-Some torque control approaches try to cancel the nonlinearities by using feedbacks from the joint torques. However, they face some challenging problems [9].

Three customary approaches in this category:

(I) Using reaction force in the shaft bearings

(II) Prony brake method

(III) Using strain gages in rotating body

Suffer from several inherent weaknesses. The first method is involved bearing friction and windage torques, which are not avoidable. The second approach requires some additional devices, which are not convenient. Finally, the third method is expensive with difficulty of installation.

It must be emphasized that, torque-based controllers formed by fractional order differential equations, are not distinguished of these problems, although, they can provide wider options in the control design compared with the integer-order controllers [10-12]. To overcome these weaknesses, voltage control strategy was proposed [13]. This strategy is free from manipulator dynamics in a decentralized structure. All nonlinearities associated with robot dynamics are canceled by feedback linearization through feedbacks from motor currents. Following this strategy, robust control of flexible-joint robots was then developed [14-15]. However, fractional order form of them remains as an open problem. The considerable point, common in all aforementioned control strategies is performing the control laws in the joint space (JS), while the goal of many usual robotic tasks is to drive the tool center point of the arm to follow a desired path in the task space (TS). Thus, despite of well behavior of JS control strategies, none of them can provide satisfactory tracking performances in TS under the imperfect transformation of control space. Some of these reasons are as follow:

-The robot's kinematics and dynamics change when a manipulator picks up different tools of unknown length or unknown gripping points [16]. Therefore, the desired joint angles, their velocities, and accelerations are not produced precisely in JS under the imperfect transformation from TS to JS.

-Tracking errors appear in TS while actuators operate in JS. Thus, transforming of control space should be carried out to perform a control law [17]. As a result, the control inputs involve errors if we use the imperfect transformation.

-The produced TS tracking errors are not detectable and compensable appropriately due to lack of feedbacks from the end-effector.

To deal with this problem, TS controllers were then developed using assumption of perfect transformation of control spaces [18-23]; however, there are still problems arises from TS dynamic formulation of robot manipulators, that involves strong couplings between the joint motions, the time derivative of jacobian matrix, as well as its inverse transformation.

Due to aforementioned problems, raised from torque-based TS control strategies, a robust fractional-order controller is proposed that is free from manipulator dynamics. The proposed approach includes two interior loops. The inner loop controls the motor position using sliding mode control (SMC) technique, while the outer loop generates a desired motor position for the inner loop by a simple fractional PID^{γ} controller. The contributions of this paper are as follows. In section 2 we recall some basic relationships for describing fractional order calculus. Nonlinear dynamic description is studied in Section 3. The overall control structure of the robust JS control design will be outlined in Section 4 and the closed-loop system stability is then presented in Section 5. An extension of the proposed JS control strategy is presented in Section 6. In Section 7 the validity of the proposed method is verified by computer simulation. Finally, we give our conclusion remarks in Section 8.

2. Fractional calculus

In this section, some basic definitions related to fractional calculus are presented. Fractional calculus is a generalization of integration and differentiation to fractional order fundamental operator ${}_aD_t^\gamma$ defined as [24]

$$ {}_aD_t^\gamma = \begin{cases} \dfrac{d^\gamma}{dt^\gamma} & ,\gamma > 0 \\ 1 & ,\gamma = 0 \\ \displaystyle\int_a^t (d\tau)^{-\gamma} & ,\gamma < 0 \end{cases} \tag{1} $$

Where a and t are the bounds of the operation and $\gamma \in \Re$. There are three definitions of fractional integration and differentiation. The most often used are the Grunwald-Letnikov (GL) definition, the Reimann-Liouville (RL) and the Caputo definition [25]. The GL definition is as:

$$ f(t) = \lim_{\substack{h\to 0 \\ nh = t-a}} h^{-\gamma} \sum_{j=0}^{n} (-1)^j \binom{\gamma}{j} f(t - jh) \tag{2} $$

Where $f(t)$ is an arbitrary differentiable function. In addition, the RL definition is formulated as

$$ {}_aD_t^\gamma f(t) = \frac{1}{\Gamma(n-\gamma)} \frac{d^n}{dt^n} \int_a^t \frac{f(\tau)}{(t-\tau)^{\gamma-n+1}} d\tau \tag{3} $$

For $(n-1 < \gamma < n)$, with $\Gamma(n)$ denoting the famous Gamma function, which is defined as

$$ \Gamma(n) = \int_a^\infty t^{n-1} e^{-\tau} d\tau \tag{4} $$

Moreover, the Caputo's definition can be written as:

$$ {}_aD_t^\gamma f(t) = \frac{1}{\Gamma(\gamma-n)} \int_a^t \frac{f^{(n)}(\tau)}{(t-\tau)^{\gamma-n+1}} d\tau \tag{5} $$

For $(n-1 < \gamma < n)$. Due to lack of space, further information about various approaches to fractional-order differentiation and integration can be found in the available literatures on this topic [25-27]. Nonlinear dynamic description is studied in the next section.

3. Dynamics of flexible joint electrically driven robot

The equations of motion for n-link flexible-joint robotic manipulator actuated by geared permanent magnet DC motors can be described as [28]

$$ D(q)\ddot{q} + C(q,\dot{q})\dot{q} + g(q) = K(r\theta - q) \tag{6} $$

$$J_m\ddot{\theta}+B_m\dot{\theta}+rK(r\theta-q)=k_mI \tag{7}$$

$$L\dot{I}+RI+k_b\dot{\theta}+\phi(t)=u \tag{8}$$

Where $q\in\Re^n$ and $\theta\in\Re^n$ represent the link angles and motor shaft angles, respectively, $D(q)\in\Re^{n\times n}$ is the symmetric positive definite manipulator inertia matrix, $\boldsymbol{C}(\boldsymbol{q},\dot{\boldsymbol{q}})\dot{\boldsymbol{q}}\in\Re^{\boldsymbol{n}}$ is a vector function containing Coriolis and centrifugal forces, $\boldsymbol{g}(\boldsymbol{q})\in\Re^{\boldsymbol{n}}$ is a vector function containing of gravitational forces, $\boldsymbol{K}\in\Re^{\boldsymbol{n\times n}}$ is a diagonal positive definite matrix representing the joint stiffness, $\boldsymbol{r}$ is an n×n transmission matrix , $\boldsymbol{J_m}\in\Re^{\boldsymbol{n\times n}}$ is a diagonal matrix of the lumped actuator rotor inertias, $\boldsymbol{B_m}\in\Re^{\boldsymbol{n\times n}}$ is diagonal matrix of the lumped actuator damping coefficients, $\boldsymbol{k_m}\in\Re^{\boldsymbol{n\times n}}$ is an invertable constant diagonal matrix characterizing the motor torque constants, $\boldsymbol{I}\in\Re^{\boldsymbol{n}}$ is the armature current vector, $\boldsymbol{L}\in\Re^{\boldsymbol{n\times n}}$ is a constant diagonal matrix of electrical inductance, $\boldsymbol{R}\in\Re^{\boldsymbol{n\times n}}$ is diagonal matrix of armature resistances, $\boldsymbol{k_b}\in\Re^{\boldsymbol{n\times n}}$ is a diagonal constant matrix for the back-emf effects, $\boldsymbol{u}\in\Re^{\boldsymbol{n}}$ is the control input voltage applied for the joint actuators, and $\boldsymbol{\phi}(t)$ represents an external disturbance.

For the convenience of representations, introduce the state variables $\boldsymbol{x}_1=\boldsymbol{q}$, $\boldsymbol{x}_2=\dot{\boldsymbol{q}}$, $\boldsymbol{x}_3=\boldsymbol{\theta}$, $\boldsymbol{x}_4=\dot{\boldsymbol{\theta}}$ and $\boldsymbol{x}_5=\boldsymbol{I}$. Thus, the motion equations (6)-(8) can be rewritten in the following state-space representation

$$\dot{\mathbf{x}}=\boldsymbol{f}(\mathbf{x})+\mathbf{B}\boldsymbol{u}-\mathbf{B}\boldsymbol{\phi}(\boldsymbol{t}) \tag{9}$$

Where

$$\boldsymbol{f}(\mathbf{x})=\begin{bmatrix}\boldsymbol{x}_2\\ \boldsymbol{D}^{-1}(\boldsymbol{x}_1)\left(-\boldsymbol{C}(\boldsymbol{x}_1,\boldsymbol{x}_2)\boldsymbol{x}_2-\boldsymbol{g}(\boldsymbol{x}_1)+\boldsymbol{K}(\boldsymbol{r}\boldsymbol{x}_3-\boldsymbol{x}_1)\right)\\ \boldsymbol{x}_4\\ \boldsymbol{J_m}^{-1}\left(-\boldsymbol{B_m}\boldsymbol{x}_4+\boldsymbol{r}\boldsymbol{K}(\boldsymbol{x}_1-\boldsymbol{r}\boldsymbol{x}_3)+\boldsymbol{k_m}\boldsymbol{x}_5\right)\\ -\boldsymbol{L}^{-1}\left(\boldsymbol{R}\boldsymbol{x}_5+\boldsymbol{k_b}\boldsymbol{x}_4\right)\end{bmatrix},\qquad \mathbf{B}=\begin{bmatrix}0 & 0 & 0 & 0 & \boldsymbol{L}^{-1}\end{bmatrix}^{\boldsymbol{T}} \tag{10}$$

4. Robust joint space control design

In this section, we are interested in deriving a decentralized control law such that in the closed-loop system, the link angles track the desired trajectory with an acceptable error. For this purpose, we design a controller that includes two interior loops. The inner loop controls the motor position using SMC technique, while the outer loop generates a desired motor position θ_d for the inner loop by a simple fractional PID$^{\gamma}$ controller.

4.1 Inner loop control design

Suppose that, the electrical subsystem of the actuator's dynamic can be rewritten as follows

$$\hat{R}I + \hat{k}_b\dot{\theta} + \eta(t) = u \tag{11}$$

Where $\hat{(\cdot)}$ denotes nominal value of $(\cdot)$, and

$$\eta(t) = L\dot{I} + (R - \hat{R})I + (k_b - \hat{k}_b)\dot{\theta} + \phi(t) \tag{12}$$

It is the disturbance. Let us define a switching surface S_θ as

$$S_\theta = e(t) + c_1\int_0^t e(\tau)d\tau \quad , \quad t \geq 0 \tag{13}$$

With $e(t) = \theta_d - \theta$, and c_1 being a positive constant. This choice of sliding surface is preferred since it is linear and it will result in a relative degree one dynamic. Now, it must be founded a control input u such that, the motor state trajectory converges to the switching surface. Toward this end, differentiating S_θ with respect to time yields

$$\dot{S}_\theta = \dot{\theta}_d - \hat{k}_b^{-1}u + \hat{k}_b^{-1}\hat{R}I + \hat{k}_b^{-1}\eta(t) + c_1e(t) \tag{14}$$

Thus, the inner loop controller can be designed as

$$u = \hat{R}I + \hat{k}_b\dot{\theta}_d + \hat{k}_bc_1e(t) + \rho sign\left(S_\theta\right) \tag{15}$$

Where ρ is a positive real constant which is determined based on bounding function on the uncertainties.

Proof: First define a non-negative function as

$$V = \frac{1}{2}S_\theta^2 \geq 0 \tag{16}$$

Differentiating (16) respect to time, and using (14) and (15) we obtain

$$\dot{V} = S_\theta\dot{S}_\theta = S_\theta\hat{k}_b^{-1}\left(\eta(t) - \rho sign\left(S_\theta\right)\right) \leq \left|S_\theta\right|\hat{k}_b^{-1}\left(\left|\eta(t)\right| - \rho\right) \tag{17}$$

Now, the sufficient condition to establish $\dot{V} < 0$ is

$$\left|\eta(t)\right| < \rho \tag{18}$$

Thus, with the controller (15), the sliding surface becomes attractive. It must be emphasized that, by choosing the control law in the form (15), chattering phenomena will occurs as soon as the state-trajectory hits the sliding surface, because of discontinuity in signum function. To reduce this effect, the following saturation function has been known to be useful in many applications

$$sat(\cdot) = \begin{cases} sign(\cdot) & \left|\cdot\right| \geq 1 \\ (\cdot) & \left|\cdot\right| < 1 \end{cases} \tag{19}$$

Hence, the input voltage u defined in (15) is modified as

$$u = \hat{R}I + \hat{k}_b\dot{\theta}_d + \hat{k}_bc_1e(t) + \rho sat\left(\frac{S_\theta}{\varepsilon}\right) \tag{20}$$

Where $\varepsilon > 0$ denotes a small design constant, called the boundary layer of the sliding surface. This completes stability proof for inner loop control design.

Remark 1: Compared with traditional torque-based SMC design, the proposed voltage-based SMC strategy doesn't require to any prior-knowledge about manipulator dynamic and bounding functions on the robot parameters and uncertainties. In fact, the motor's current includes the effects of nonlinearities and coupling in the robot manipulator.

4.2 Outer loop control design

Here, the control objective is to design a desired trajectory θ_d for the inner loop controller, so that $\theta \to \theta_d$ which further implies convergence of q to the desired trajectory q_d. Based on this observation, the outer loop is formed for tracking the joint position by suggesting

$$\theta_d = K_d D^{\gamma} E(t) + K_p E(t) + K_I \int_0^t E(\sigma) d\sigma \quad , \quad t \geq 0 \tag{21}$$

Where K_d, γ, K_p, and K_I are the design parameters and

$$E(t) = q_d - q \tag{22}$$

Represent link position tracking error. Now, the voltage of every motor should be limited to protect the motor against over voltages. Therefore, by using a voltage limiter, we obtain

$$u(t) = v \qquad , \qquad \text{for } |v| \leq v_{\max} \tag{23}$$

$$u(t) = v_{\max} \text{sign(v)} \quad , \quad \text{for } |v| > v_{\max} \tag{24}$$

Where $v_{\max}$ a positive constant is called as the maximum permitted voltage of motor and v is expressed as

$$v = \hat{R} I + \hat{k}_b \dot{\theta}_d + \hat{k}_b c_1 e(t) + \rho sat\left(\frac{S_\theta}{\varepsilon}\right) \tag{25}$$

5. Stability analysis

Due to decentralized structure of the proposed controller, stability analysis is presented separately for every individual joint to verify stability of the robotic system. To this end, some assumptions are assumed to be valid throughout this paper:

Assumption 1: The control law given by (23)-(25) implies that the motor voltage is limited, that is

$$|u(t)| \leq v_{\max} \tag{26}$$

Assumption 2: The JS desired trajectory q_d, the TS desired trajectory X_d and their derivatives up to a necessary order are available and all uniformly bounded.

Assumption 3: The external disturbance $\phi(t)$ is bounded as

$$|\phi(t)| \leq \phi_{\max} \tag{27}$$

Where $\phi_{\max}$ is a positive constant.

Since, the control laws given by (23)-(25), operate in two areas, i.e., $|v| \leq v_{\max}$ and $|v| > v_{\max}$, therefore stability analysis, and tracking performance should be evaluated in both areas.

5.1 Area of $|v| \le v_{\max}$

In this area, we have

$$u(t) = \hat{R}I + \hat{k}_b \dot{\theta}_d + \hat{k}_b c_1 e(t) + \rho sat\left(\frac{S_\theta}{\varepsilon}\right) \tag{28}$$

Substituting the above equation into (11), rearranging with some mathematical simplification yields the error dynamic equation as

$$\dot{e}(t) + c_1 e(t) = \hat{k}_b^{-1}\left(\eta(t) - \rho sat\left(\frac{S_\theta}{\varepsilon}\right)\right) \tag{29}$$

The variables $\dot{\theta}$, I, and $\dot{I}$ are bounded, since u is bounded [15]. These results, in addition to Assumption 3, obtains the function bounding the RHS of equation (29) as

$$\hat{k}_b^{-1}\left|\eta(t) - \rho sat\left(\frac{S_\theta}{\varepsilon}\right)\right| \le \hat{k}_b^{-1}\left(L\dot{I}_{\max} + \zeta_1 I_{\max} + \zeta_2 \dot{\theta}_{\max} + \phi_{\max} + \rho\right) = \psi \tag{30}$$

Where $(\bullet)_{\max}$ is a positive scalar function, representing the upper bound of $(\bullet)$, and ζ_1 and ζ_2 are positive constants and the upper bound of $(R - \hat{R})$ and $(k_b - \hat{k}_b)$, respectively. Thus, according to (29), $e(t)$ and $\dot{e}(t)$ are bounded, which also means boundededness of $\dot{\theta}_d$, whereas $\dot{\theta}$ and $\dot{e}(t)$ are bounded. By using (21), it is also verify that

$$K_d D^{1+\gamma} E(t) + K_p \dot{E}(t) + K_I E(t) = \dot{\theta}_d \tag{31}$$

Which is a fractional order linear system with limited input $\dot{\theta}_d$. It can be easily show that, the output of $E(t)$ is bounded under limited input $\dot{\theta}_d$, if the fractional order linear system (31) be strictly stable. To this end we utilizes the following lemma from [29]

Lemma: The system is BIBO stable, if

$$\left|\arg(\omega_i)\right| > \frac{\alpha\pi}{2} \tag{32}$$

Where $\omega = s^\alpha, \alpha \in \Re^+, 0 < \alpha < 2$, and ω_i is the i[th] root of denominator of transfer function $E(s)/\dot{\theta}_d(s)$.

Proof: For stability analysis, generally, we derive the transfer function and then we study the location of the roots of the denominator. The transfer function is stable if the roots are in LHP [29]. Hence, the transfer function is in the form:

$$G(s) = \frac{E(s)}{\dot{\theta}_d(s)} = \frac{1}{K_d s^{1+\gamma} + K_p s + K_I} \tag{33}$$

According to [29], every fractional order system can be expressed in commensurate form, in which the domain of the $G(s)$ definition is a Riemann surface with ϑ Riemann sheets, i.e.

$$G(s) = \frac{1}{K_d s^{\vartheta_1/\vartheta} + K_p s^{\vartheta_2/\vartheta} + K_I} \tag{34}$$

Where ϑ_1, ϑ_2 and ϑ are integers, and ϑ is the least common multiple of $1+\gamma$ and 1. Therefore, using the procedure explained in [29, 30] we can choosing the control parameters γ, K_d, K_p and

K_I such that, the closed loop poles to be in desired places, that means boundedness of E. From (22) and according to assumption 2, boundedness of q can be achieved. Also, from (7), we have

$$J_m\ddot{\theta} + B_m\dot{\theta} + r^2K\theta = k_m I + rKq \tag{35}$$

Which represent a stable 2nd order LTI system driven by the bounded input $k_m I + rKq$. Thus θ, $\dot{\theta}$ and $\ddot{\theta}$ are bounded. From boundedness of θ and $e(t)$, it can be founded that θ_d is bounded. Thus, with the same manipulation similar to (33) and (34), boundedness of $\dot{E}(t)$ can be achieved that means boundedness of $\dot{q}$, whereas the desired trajectory $\dot{q}_d$ is bounded. Now, since all states $\theta, \dot{\theta}, q$, $\dot{q}$ and I associated with each joint are bounded, then vectors $\boldsymbol{\theta}$, $\dot{\boldsymbol{\theta}}$, $\boldsymbol{q}$, $\dot{\boldsymbol{q}}$ and $\boldsymbol{I}$ are bounded. As a result, the robotic system has the Bounded Input-Bounded Output (BIBO) stability.

5.2 Area of $|v| > v_{\max}$

In this area, we have

$$L\dot{I} + RI + k_b\dot{\theta} + \phi(t) = v_{\max}\text{sign}(v) \tag{36}$$

To consider the convergence of tracking error $e(t)$ in this area, a positive definite function is proposed as

$$V = \frac{1}{2}k_b e^2(t) \geq 0 \tag{37}$$

The differentiation of V is

$$\dot{V} = k_b e(t)\dot{e}(t) \tag{38}$$

From $e(t) = \theta_d - \theta$ and using (36), we have

$$\dot{V} = e(t)\left(k_b\dot{\theta}_d + L\dot{I} + RI + \phi(t) - v_{\max}\text{sign}(v)\right) \tag{39}$$

Assume that, there exists a positive scalar denoted by σ that

$$\left|L\dot{I} + RI + k_b\dot{\theta}_d + \phi(t)\right| < \sigma \tag{40}$$

Thus, to establish the convergence, $\dot{V} < 0$, it is sufficient that

$$v_{\max}\text{sign}(v) = \sigma\text{sign}(e) \tag{41}$$

Proof: Substituting (41) into (39) yields

$$\dot{V} = e(t)\left(k_b\dot{\theta}_d + L\dot{I} + RI + \phi(t) - \sigma\text{sign}(e)\right) \tag{42}$$

Now, for $\dot{V}$ to be a negative definite function, the requirement is (40)

$$\begin{aligned}\dot{V} &\leq |e(t)|\left|k_b\dot{\theta}_d + L\dot{I} + RI + \phi(t)\right| - \sigma e(t)\text{sign}\left(e(t)\right)\\ &= |e(t)|\left|L\dot{I} + RI + \phi(t) + k_b\dot{\theta}_d\right| - \sigma|e(t)|\\ &= |e(t)|\left(\left|L\dot{I} + RI + \phi(t) + k_b\dot{\theta}_d\right| - \sigma\right)\end{aligned} \tag{43}$$

Thus, the motor tracking error is converged until the control system comes into the area governed by control law (23). As a result, even if the robotic system starts from the area of $|v| > v_{\max}$, it goes into the area of $|v| \le v_{\max}$, that all states are bounded. Equation (41) means that

$$v_{\max} = \sigma \tag{44}$$

Therefore, the maximum voltage of motor should satisfy (44) for the convergence of motor position tracking error $e(t)$. From the closed loop system (36), we can obtain

$$L\dot{I} + RI = v_{\max}\text{sign}(v) - k_b\dot{\theta} - \phi(t) \tag{45}$$

The RHS of (45) is bounded as

$$\left|v_{\max}\text{sign(v)} - k_b\dot{\theta} - \phi(t)\right| \le v_{\max} + k_b\dot{\theta}_{\max} + \phi_{\max} \tag{46}$$

Thus, from (45), it is guaranteed that output I is bounded. From boundedness of I, one can imply that, the linear stable system (35) is bounded under bounded input $k_m I + rKq$ which result in boundedness of variables θ, $\dot{\theta}$, and $\ddot{\theta}$. With the same procedure as (33) and (34), boundedness of $\dot{E}$ and so $\dot{q}$ can be derived. Since all states θ, $\dot{\theta}$, q, $\dot{q}$ and I associated with each joint are bounded then vectors $\boldsymbol{\theta}$, $\dot{\boldsymbol{\theta}}$, $\boldsymbol{q}$, $\dot{\boldsymbol{q}}$ and $\boldsymbol{I}$ are bounded. Thus, the robotic system has the Bounded Input-Bounded Output (BIBO) stability.

6. Robust task space control design

As mentioned before, despite of well behavior of JS control strategies, none of them can provide satisfactory tracking performances in TS under the imperfect transformation from Cartesian to joint angles. For this reason, here, we will improve the outer-loop of the aforementioned JS controller to track a desired trajectory in TS. Let us $X \in \Re^n$ to be a TS vector, representing the position and orientation of the robot end-effecor relative to a fixed user defined reference frame. Then, the forward kinematic and differential kinematic transformation between the robot links coordinates and the end-effector coordinates can be written as

$$X = h(q) \tag{47}$$

$$\dot{X} = J(q)\dot{q} \tag{48}$$

Where $h(q): \Re^n \to \Re^n$ is the differentiable forward kinematics of the manipulator, and $J(q) \in \Re^{n\times n}$ denotes the Jacobian matrix defined as $J(q) = \partial h(q)/\partial q \in \Re^{n\times n}$. Let us define the TS tracking error as

$$E_x = X_d - X \tag{49}$$

Where, X_d is the desired TS position vector. Now, we propose the outer-loop controller in the form

$$\theta_d = \int_0^t \hat{J}^{-1}(q)\left(K_d D^{1+\gamma}E_x(\tau) + K_p\dot{E}_x(\tau) + K_I E_x(\tau)\right)d\tau \quad , \text{t} \ge 0 \tag{50}$$

A block diagram of the proposed control approach is depicted in Figure 1. By stability analysis, similar to previous section, we show the closed-loop system stability. Toward this end, tracking performance is evaluated in both areas.

6.1 Area of $|v| \le v_{\max}$

As was done in previous section, one can show that the RHS of (29), $e(t)$ and so $\dot{e}(t)$ are bounded. Thus, boundedness of $\dot{\theta}_d$ can be achieved. Differentiating both sides of (50) with respect to time gives

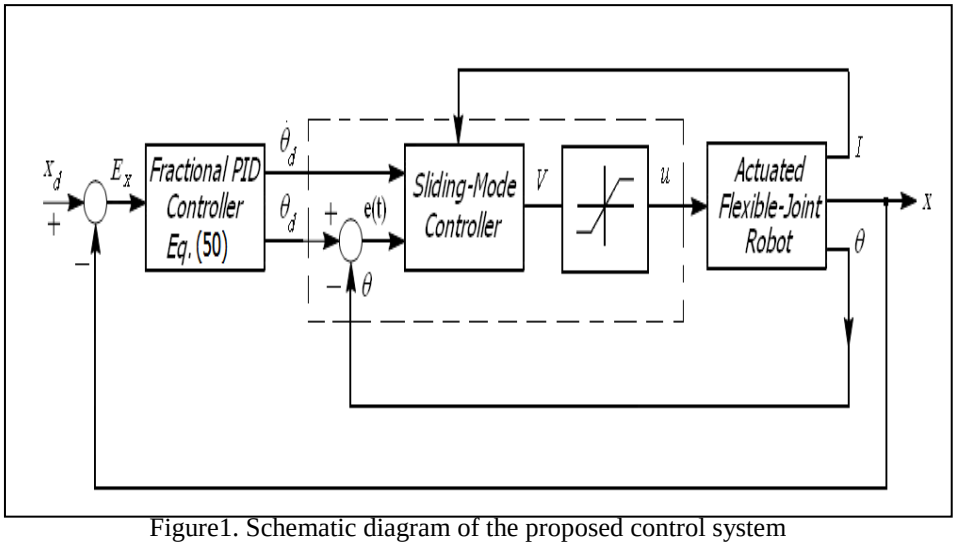

Figure1. Schematic diagram of the proposed control system

$$K_d D^{1+\gamma} E_x + K_p \dot{E}_x + K_I E_x = \hat{J}\dot{\theta}_d \qquad (51)$$

Which is a fractional order linear system with limited input $\hat{J}\dot{\theta}_d$, whereas $\hat{J}$, and $\dot{\theta}_d$ are bounded. By the same analysis similar to section 5.1, we can obtain boundedness of E_x, and so X, which in turn means boundedness of q according to (47). As a conclusion of this analysis, the robotic system has the BIBO stability in this area, since all of system states are bounded.

6.2 Area of $|v| > v_{\max}$

It can be easily show that, by choosing a positive definite function, as (37), starting from an arbitrary initial $e(0)$ under the condition (44), concludes reducing the value of $|e(t)|$. Thus, motor voltage will move to the area of $|v| \le v_{\max}$ which all signals are bounded. As a result of this discussion, boundedness of θ, $\dot{\theta}$, $\ddot{\theta}$, and I can be achieved as same as before. Rewrite Equation (51) as a fractional commensurate form as (34) with limited input $\hat{J}(q)\dot{\theta}_d$. Thus, E_x, and $\dot{E}_x$ are bounded. From $E_x = X_d - X$, $\dot{E}_x = \dot{X}_d - \dot{X}$, and using Assumption 2, it follows that X, and $\dot{X}$ are bounded. This completes the proof of the closed-loop system stability. As a conclusion of this analysis, the robotic system has the BIBO stability.

7. Computer simulation

The robust performance of the proposed control strategy was verified through simulations of a two-link electrically driven robot manipulator with flexible joints, uncertainties in the motor dynamics and without requiring the information of manipulator dynamic. The parameters for the motion equations in the form (6) with link masses m_1, m_2, lengths l_1, l_2, link angular positions q_1, q_2, and link's moment of inertia I_1, I_2 are

$$D(q)=\begin{bmatrix} d_{11} & d_{12} \\ d_{21} & d_{22} \end{bmatrix},\ C(q,\dot{q})\dot{q}=\begin{bmatrix} -2m_2 l_1 l_{c2} sin(q_2)\left(\dot{q}_1\dot{q}_2+0.5\dot{q}_2^2\right) \\ m_2 l_1 l_{c2} sin(q_2)\dot{q}_1^2 \end{bmatrix}$$
$$g(q)=\begin{bmatrix} (m_1 l_{c1}+m_2 l_1)\, g cos(q_1)+m_2 l_{c2} g cos(q_1+q_2) \\ m_2 l_{c2} g cos(q_1+q_2) \end{bmatrix} \quad (52)$$
$$d_{11}=m_2\left(l_1^2+l_{c2}^2+2l_1 l_{c2} cos(q_2)\right)+m_1 l_{c1}^2+I_1+I_2$$
$$d_{21}=d_{12}=m_2 l_{c2}^2+m_2 l_1 l_{c2} cos(q_2)+I_2$$
$$d_{22}=m_2 l_{c2}^2+I_2$$

Where l_{ci} represent the distance between the center of mass of link and the i[th] joint. For the convenience of simulation, the nominal parameters are given as $l_1=l_2=1m$, $l_{c1}=l_{c2}=0.5m$, $m_1=15kg$ and $m_2=6kg$, $I_1=5\ kg.m^2$ and $I_2=2\ kg.m^2$; Also, the exact-actuator dynamic model parameters are selected as $R=diag(1.6,1.6)\Omega$, $k_m=k_b=diag(0.26,0.26)$(Nm/A), $L=diag(10^{-3},10^{-3})$ (H), $J_m=diag(2\times10^{-4},2\times10^{-4})(kg.m^2)$, $B_m=diag(10^{-3},10^{-3})$(Nm.sec/rad), $K=diag(500,500)$(Nm/rad), and $r=diag(0.02,0.02)$. Let the desired trajectory be a circular path specified by 0.15m radius centered at (0.35m, 0.35m), in the TS. The forward kinematic equation is given by

$$X=\begin{cases} l_1 cos(q_1)+l_2 cos(q_1+q_2) \\ l_1 sin(q_1)+l_2 sin(q_1+q_2) \end{cases} \quad (53)$$

The manipulator Jacobian matrix $J(q)$ mapping from TS to JS is given by

$$J(q)=\begin{bmatrix} -l_1 sin(q_1)-l_2 sin(q_1+q_2) & -l_2 sin(q_1+q_2) \\ l_1 cos(q_1)+l_2 cos(q_1+q_2) & l_2 cos(q_1+q_2) \end{bmatrix} \quad (54)$$

The link's length is estimated by a gain of 0.9 from real values and initial tracking errors are considered zero in all simulations. Now, due to clarify the significance of the proposed controller two-simulation set will be investigated.

Simulation 1: The JS controller given by (23)-(25) are simulated to track a circle in TS, with %10 uncertainty in motor and link parameters, without any knowledge of manipulator dynamic. We set the controller parameters as $c_1=50$, $K_d=70$, $K_p=1400$, $\gamma=0.8$, $K_I=2000$ and $\varepsilon=0.2$. In order to stability analysis of transfer function (33), we use the characteristic equation of (33) in the form

$$70s^{1.8}+1400s+2000=0 \tag{55}$$

Mapping the poles from s^q-plane into the w-plane yields:

$$70w^{9}+1400w^{5}+2000=0 \tag{56}$$

Where $w=s^{1/m}$, and $m=5$ represents the sheets number of the Riemann surface. Solving the polynomial (56) we get the following roots and their absolute phase:

$$\begin{aligned}
&w_{1,2}=1.4768\pm 1.4961\mathrm{i} && , \quad \left|\arg(w_{1,2})\right|=0.7919\\
&w_{3,4}=-1.5125\pm 1.496\mathrm{i} && , \quad \left|\arg(w_{3,4})\right|=2.3617\\
&w_{5,6}=0.8842\pm 0.6303\mathrm{i} && , \quad \left|\arg(w_{5,6})\right|=0.6193\\
&w_{7,8}=-0.3181\pm 1.0202\mathrm{i} && , \quad \left|\arg(w_{7,8})\right|=1.873\\
&w_{9}=-1.0608 && , \quad \left|\arg(w_{9})\right|=3.1416
\end{aligned} \tag{57}$$

It can be easily shown that, only the complex conjugate roots $w_{5,6}$, are exist in the first Riemann sheet, expressed by $\left|\arg(w)\right|<\pi/m$, which satisfy the stability condition given as $\left|\arg(w)\right|>\pi/2m=0.3142$. It means that, system (55) is stable. By this definition, the tracking performance using the above proposed scheme is plotted in Figure 2. Figures 3 and 4 are shown the norm of tracking errors in both TS and JS respectively. From the plots, we see that in the steady state, the norm of TS tracking error has a maximum value of about 7cm, while the norm of JS tracking errors are less than 7×10^{-3} rad which is negligible. Thus, despite of good tracking performance of the robust JS control strategies in JS, shown by Figure 5, they cannot provide satisfactory performance in TS under imperfect transformation of control space. The control signals at both joints are plotted in Figure 6. As a result, the performance of the JS control strategies is degraded by the imperfect transformation.

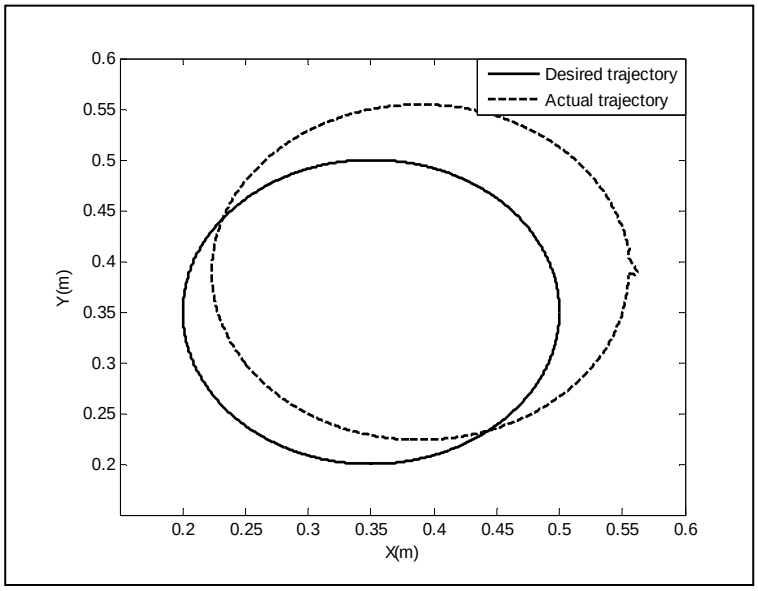

Figure2. Tracking performance in TS

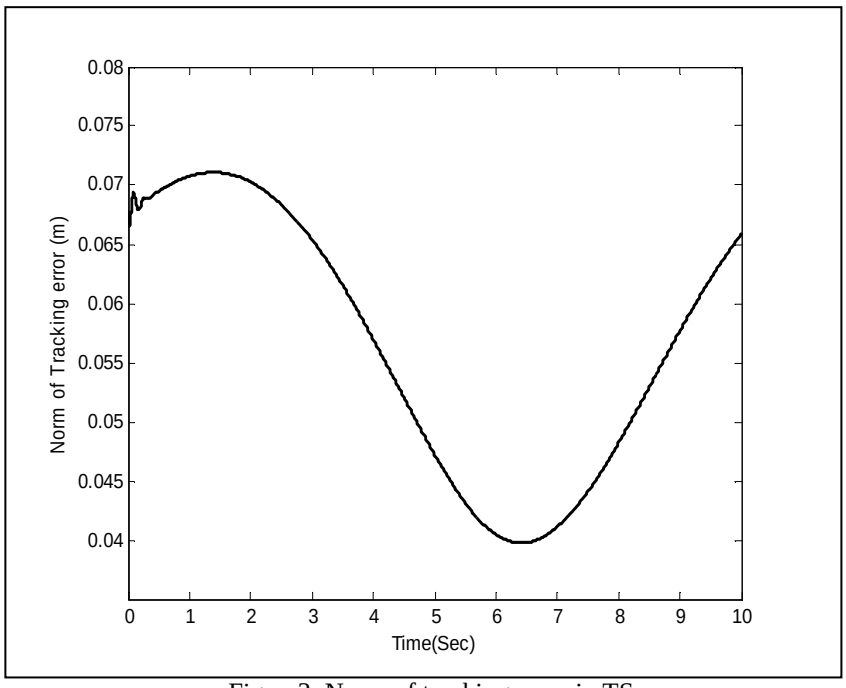

Figure3. Norm of tracking error in TS

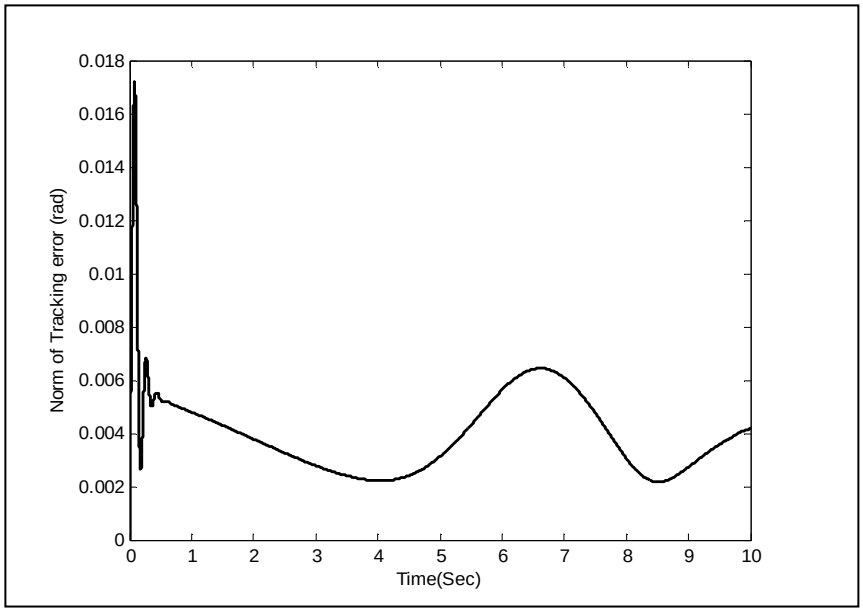

Figure4. Norm of tracking error in JS

Simulation 2: The TS control given by (23)-(25) and (50) are simulated. The control parameters set as $c_1 = 10$, $K_d = 90$, $K_p = 1000$, $K_I = 2000$, $\gamma = 0.6$ and $\varepsilon = 0.2$. Figure 7 shows the end-effector position of robot manipulator in the x-y-directions under uncertainties similar to simulation 1. As can be seen from Figure 8, end-effector position converges nicely to the desired value in TS. The profile of actuator voltage is shown in Figure 9. Simulation results indicate that the robot's end-effector successfully follows circle trajectory, while achieving robust performance of closed loop system.

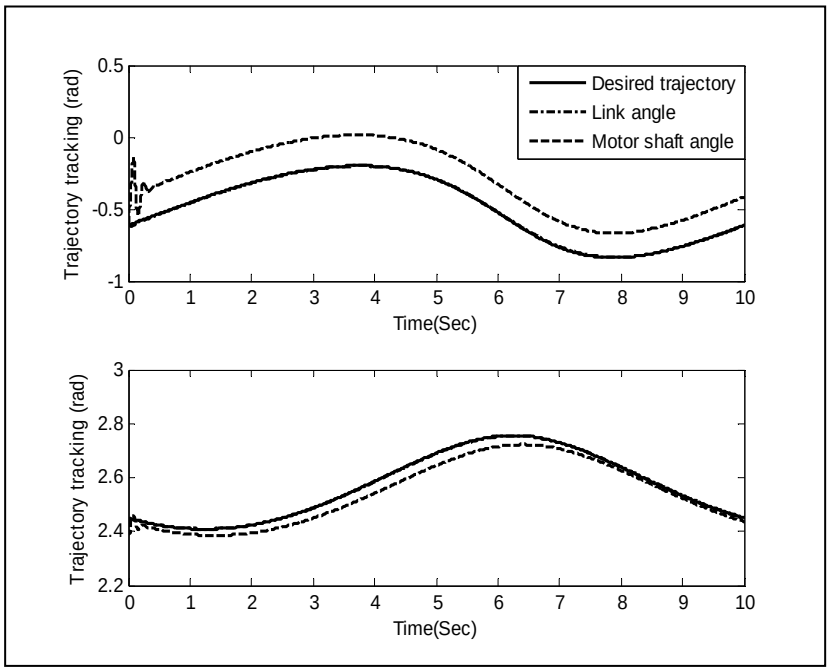

Figure5. Tracking performance in JS

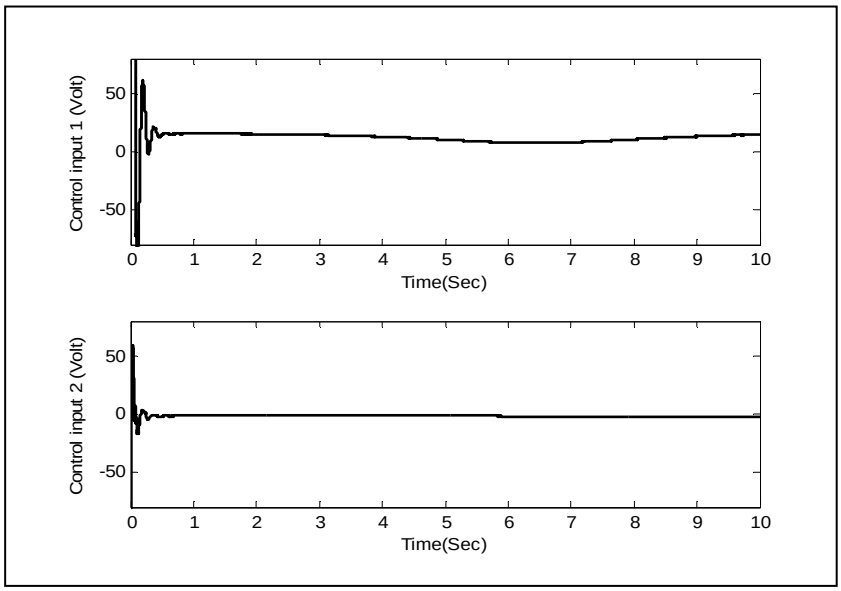

Figure6. The control efforts for both joints

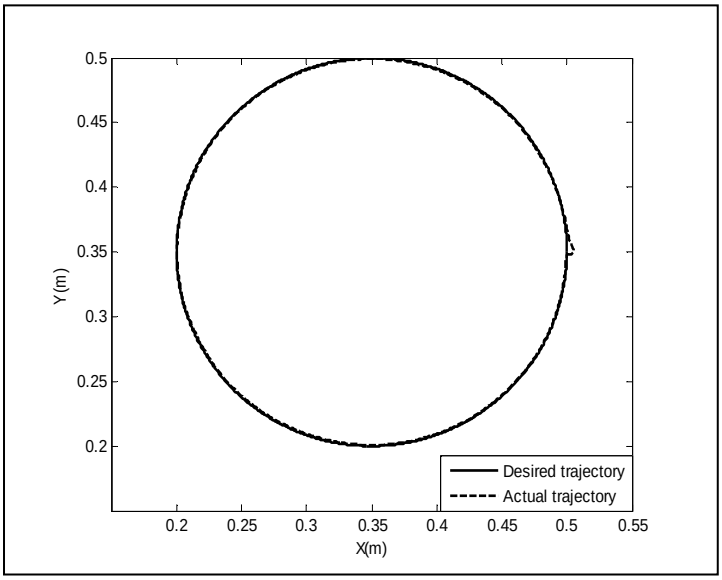

Figure7. Tracking performance in TS

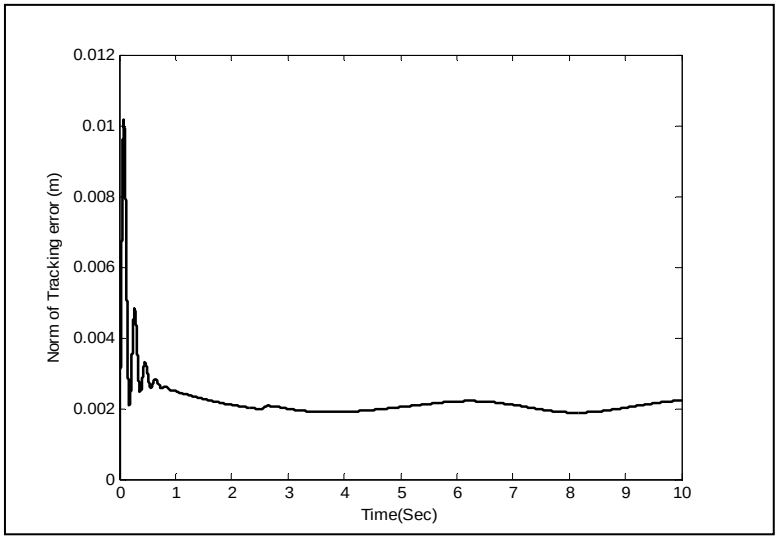

Figure8. Norm of tracking error in TS

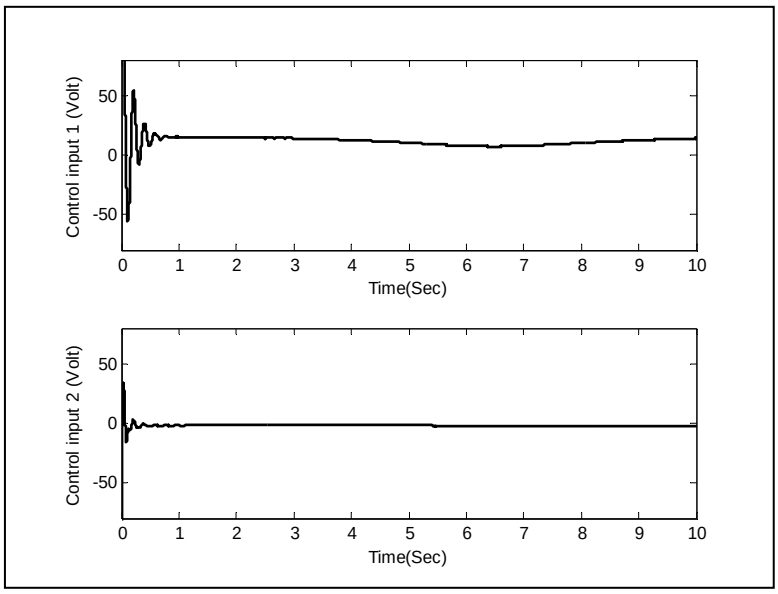

Figure9. The control efforts for both joints

8. Conclusion

Many robust control techniques have been designed to control of robot manipulator in JS. However, control performance is degraded under imperfect transformation of control space from TS to JS. In this paper a robust fractional-order control has been proposed for flexible joint electrically driven robots. The proposed approach is free from robot manipulator dynamic and robust against all uncertainties in manipulator dynamics and its motors. It is shown that the robotic system has the Bounded Input-Bounded Output (BIBO) stability in the sense that all the signals are bounded. Numerical results for a two-link flexible joint robot driven by permanent magnet dc motors have shown the superiority of TS controller to the JS controller. The tracking performance is satisfactory such that the flexibility of the robotic system has been well under control. The control efforts are continuous and soft to be easily implemented. The voltages of motors are permitted under the maximum values.

9. References

[1] Melhem, K. and Wang, W. 2009. Global Output tracking control of flexible Joint Robots via actorization of the Manipulator Mass Matrix. IEEE Trans. on Robotics., 25, 428-437.

[2] Chaoui, H., Sicard, P. and Gueaieb, W. 2009. ANN-Based Adaptive Control of Robotic Manipulators with Friction and Joint Elasticity. IEEE Trans. on Industrial Electronics., 56, 3174-3187.

[3] Bang, J. S., Shim, H., Park, S. K. and Seo, J. H. 2010. Robust Tracking and Vibration Suppression for a Two-Inertia System by Combining Backstepping Approach with disturbance Observer. IEEE Trans. on Industrial Electronics., 57, 3197-3206.

[4] Talole, E., Kolhe, P. and Phadke, B. 2010. Extended state observer based control of flexible joint system with experimental validation. IEEE Trans. Ind. Electron., 57, 1411-1419.

[5] Khanesar, M. A., Kaynak, O. and Teshnehlab. M. 2011. Direct Model Reference Takagi–Sugeno Fuzzy Control of SISO Nonlinear Systems. IEEE Trans. on Fuzzy Systems., 19, 914-924.

[6] Chen, Ch. Sh. 2011. Robust Self-Organizing Neural-Fuzzy Control With Uncertainty Observer for MIMO Nonlinear Systems. IEEE Trans. on Fuzzy Systems., 19, 694-706.
[7] Chang, Y. C., and Yen, H. M. 2011. Design of a Robust Position Feedback Tracking Controller for Flexible-Joint Robots., IET Control Theory Appl., 5, 351-363.
[8] Izadbakhsh, A. and Fateh, M. M. 2014. Robust Lyapunov-based control of flexible-joint robots using voltage control strategy. Arabian journal for science and Engineering. 39: 3111-3121. DOI 10.1007/s13369-014-0949-2.
[9] Izadbakhsh, A. and Rafiei, S.M.R. 2009. Endpoint Perfect Tracking Control of Robots - A Robust Non Inversion-Based Approach. International Journal of Control, Automation, and Systems, 7(6), 888-898.
[10] Fonseca Ferreira, N. M., Tenreiro Machado, J. A. and Boaventura Cunha, J. 2001. Fractional-Order Position/Force Robot Control. Journal of Advance Computational Intelligence and intelligent informatics., 9, 379-386.
[11] Petras, I. 2009. Fractional Order Feedback Control of a DC Motor. Journal of Electrical Engineering., 60, 117–128.
[12] Delavari, H., Ghaderi, R., Ranjbar, A. and Momani, S. 2010. Fuzzy fractional order sliding mode controller for nonlinear systems. Communications in Nonlinear Science and Numerical Simulation., 15, 963-978.
[13] Fateh, M. M. 2008. On the Voltage-Based Control of Robot Manipulators. International Journal of Control, Automation and Systems, 6, 702-712.
[14] Fateh, M. M. 2012. Nonlinear Control of Electrical Flexible-Joint Robots. Nonlinear Dynamic., 67, 2549-2559.
[15] Fateh, M. M. 2012. Robust Control of Flexible-Joint Robots Using Voltage Control Strategy. Nonlinear Dynamic., 67, 1525-1537.
[16] Cheah, C. C., Liu, C. and Slotine, J. J. E. 2010. Adaptive Jacobian Vision Based Control for Robots with Uncertain Depth Information. Automatica., 46, 1228-1233.
[17] Moreno-Valenzuela, J., Campa, R. and Santibáñez, V. 2013. Model-based control of a class of voltage-driven robot manipulators with non-passive dynamics. Computers & Electrical Engineering, 39(7), 2086-2099.
[18] Colbaugh, R. and Glass, K. 1997. Adaptive Task-Space Control of Flexible-Joint Manipulators. Journal of Intelligent and Robotic Systems., 20, 225-249.
[19] Hu, Y-R. and Vukovich, G. 2001. Position and Force Control of Flexible Joint Robots during Constrained Motion Tasks. Mechanism and Machine Theory., 36, 853-871.
[20] Faroog, M., Wang, D. B. and Dar, N. U. 2008. Hybrid force/position control scheme for Flexible Joint Robot with Friction Between and the End-Effector and the Environment. Int. J. Eng. Sci., 46, 1266-1278.
[21] Goldsmith, P. B., Francis, B. A. and Goldenberg, A. A. 1999. Stability of Hybrid Position/Force Control Applied to Manipulators with Flexible Joints. Int. Jour. Of. Robotics and Automation., 14, 146-160.
[22] Tian, L., Wang, J. and Mao, Z. 2004. Constrained Motion Control of Flexible Robot Manipulators based on Recurrent Neural Networks. IEEE Trans. on Syst., Man Cybern., Part B., 34, 1541-1552.
[23] Tian, L. and Goldenberg, A. 1995. Adaptive and Sliding Control of Flexible Joint Robots in Constrained motion. IEEE International Conf. on Systems, Man and Cybernetics., 4161–4166.
[24] Caldero, A. J., Vinagre, B. M. and Feliu, V. 2006. Fractional order control strategies for power electronic buck converters, Signal Processing., 86, 2803-2819.
[25] Podlubny, I. 1999. Fractional Differential Equations. Academic Press. San Diego: CA.
[26] Oldham, K. B. and Spanier, J. 1974. The Fractional Calculus. Academic Press. New York.

[27] Miller, K. S. and Ross. B. 1993. An Introduction to the Fractional Calculus and Fractional Differential Equations., Wiley., New York.

[28] Spong, M. 1980. Modeling and Control of Elastic Joint Robots. Journal of Dynamic Syst. Meas., Contr., 109, 107-111.

[29] Petr´aˇs, I. 2011. Fractional-Order Nonlinear Systems, Modeling, Analysis and Simulation. Higher Education Press. Beijing and Springer-Verlag Berlin Heidelberg, (Chapter 3).

[30] Ahmed, E., El-Sayed, A. M. A. and Hala A.A. El-Saka. 2006. On some Routh–Hurwitz conditions for fractional order differential equations and their applications in Lorenz, Rössler, Chua and Chen systems. Physics Letters A., 358, 1-4.